Self-sensing hybrid composite laminate by piezoelectric nanofibers interleaving

(Article begins on next page)

19 April 2024

Self-sensing hybrid composite laminate by piezoelectric nanofibers interleaving

Tommaso Maria Brugo [a]*, Emanuele Maccaferri [b], Davide Cocchi [a],

Laura Mazzocchetti [b], Loris Giorgini [b], Davide Fabiani [c], Andrea Zucchelli [a]

[a] Department of Industrial Engineering, University of Bologna, Viale Risorgimento 2, 40136 Bologna, Italy.

[b] Department of Industrial Chemistry, University of Bologna, Viale Risorgimento 4, 40136 Bologna, Italy

[c] Department of Electrical, Electronic, and Information Engineering, University of Bologna, Viale Risorgimento 2, 40136 Bologna, Italy

*Corresponding author e-mail address: tommasomaria.brugo@unibo.it

Abstract

One of the most critical aspects of composite materials is their vulnerability to impact loadings. In recent years, Structural Health Monitoring (SHM) systems have been developed to continuously watch over on the event of an impact and so monitor the health status of the structure. However, this technique needs the integration of sensors in the composite laminate, like Fiber Bragg Grating or piezoelectric ceramic transducers, which often can dramatically reduce the inherent strength of the hosting material. The aim of this work is the integration of the composite laminate with a nanostructured piezoelectric sensor, based on PVDF-TrFE nanofibers and aluminum sheets as electrodes. Structurally, the resulting composite is a hybrid laminate known as Glass Laminate Aluminum Reinforced Epoxy (GLARE), consisting of aluminum sheets alternatively bonded to glass-epoxy prepreg layers, functionalized with PVDF-TrFE interleaved nanofibrous mats. Hence, this nanostructured hybrid laminate becomes itself a piezoelectric sensor, capable to detect impacts on its whole surface. Non-destructive impact tests were performed using an instrumented drop-weight tower to investigate the real-time electrical response of the self-sensing laminate. A lumped electric model was applied to study and optimize the circuit electrical parameters. Then, the self-sensing laminate performance were evaluated in terms of linearity and spatial uniformity.

Keywords: A. Nano-structures, A. Smart materials, B. Impact behaviour, D. Non-destructive testing, Structural Health Monitoring (SHM)

1. Introduction

The use of fiber-reinforced plastics (FRP) composite laminates is rapidly growing in different fields, such as aerospace and wind energy, thanks to their higher specific stiffness and strength compared to conventional materials. However, due to their laminar structure, they are prone to delamination and are susceptible to out-of-plane impact loads. Often, the flaw initiates and propagates inside the laminate without any visible damage on the outer surfaces, until it reaches a critical dimension that causes the sudden and catastrophic failure of the component. The safety is therefore guaranteed by over-dimensioning them and by time-consuming periodic non-destructive testing (NDT) inspections, that negatively impact on the overall weight and life-cycle cost of the structure [1,2].

To overcome these limitations, Structural Health Monitoring (SHM) systems are being developed to continuously watch over the health status of the structure during operation and immediately detect the damage. The monitoring sensors can be either externally mounted or integrated into the laminate. External sensors usually do not affect mechanical performance of the laminate, however, they are bulky and exposed to external environmental conditions, electronic interferences and impacts [1]. For this reason, efforts have been made to embed commercial sensors into the composite between the laminate plies. The most widely used are Fiber Bragg Grating (FBG) [3] and piezoelectric ceramic-based sensors, like lead zirconate titanate (PZT) wafers [4] or microfibers [5]. FBG sensors, thanks to their multiplexing capacity, allow the strain measurement on different spots along with a single optical fiber [6,7]. However, inserting a sub-millimetric optical fiber between composite plies perpendicularly to the reinforcing fiber produce an eye-shaped resin pocket defect which can cause matrix cracking and subsequent delamination [8]. Piezoelectric sensors are widely employed to measure frequency vibrations, like Lamb waves or acoustic emission, due to their reduced weight, size and cost [6]. Thanks to their high piezoelectric constant, PZT wafers show an excellent sensitivity with respect to other conventional sensors like strain gauges, fiber optics and more flexible piezoelectric polymers [9,10]. However, their ceramic inherent nature makes them extremely brittle. In fact, PZT fracture causes an interface crack nucleation, which brings to unstable delamination [11]. This aspect affects the composite fatigue strength and limits the bearing strength capacity of the laminate [12]. By changing the morphology of the PZT from wafer disks to microfibers (micro-sized lead zirconate titanate fibers) the intrusiveness of the sensor on the hosting laminate can be reduced. For instance, the laminate shear

strength is reduced by 7% by embedding PZT microfibers in unidirectional GFRP prepreg plies compared to 15% by embedding PZT disks [5]. An alternative to brittle piezoceramic sensors is polyvinylidene difluoride (PVDF) polymeric films. These have the advantages of high flexibility, low mass and cost and high internal damping [13,14]. However the interface strength between the sensor and the hosting matrix can be an issue [15,16]. Another possibility is to make the matrix system self-sensing through additives, e.g. by adding carbon nanotubes (CNTs) [17]. Compared to the previously described extrinsic sensors, that constitute a foreign body hosted in the laminate, the matrix itself when reinforced with CNTs becomes intrinsically a sensor. This concept overcomes the issues related to mechanical performance reduction [17–19]. The use of a small amount of CNTs makes the polymer matrix electrically conductive and piezo-resistive, ensuring a strict relationship between the mechanical deformations and the measured electrical resistance [20]. However, the sensing performances are susceptible to the unavoidable inhomogeneous dispersion of the filler (entanglements) within the resin, which impacts on the electrical response of the obtained nanocomposites [17,20].

In this work, the integration of a nanostructured piezoelectric sensor made by poly(vinylidenefluoride-trifluoroethylene) (PVDF-TrFE) nanofibers into a composite laminate with aluminum sheets as electrodes is proposed. Structurally, the resulting composite is a hybrid laminate consisting of aluminum sheets alternatively bonded to glass-fiber reinforced plastics (GFRP) prepreg layers and interleaved with PVDF-TrFE nanofibrous mats. Such lay-up belongs to a special class of hybrid laminates known as Glass Laminate Aluminum Reinforced Epoxy (GLARE), well known for its superior impact strength [21]. Moreover, nanofibrous mat interleaving is a consolidated technique used to increase the delamination toughness and impact strength of composite laminates without affecting the overall stiffness [22–24]. Hence, the resulting nanostructured hybrid laminate constitutes itself a piezoelectric sensor capable of detecting an impact load on its whole surface, with potentially superior impact resistance compared to pristine ones.

2. Materials & Methods

2.1. Fabrication process of the self-sensing laminate

2.1.1. Piezoelectric polymer and electrospinning

The piezoelectric nanofibrous non-woven mat was fabricated by electrospinning method (Fig. 1a) and nanofibers were made of PVDF-TrFE 70:30 mol % copolymer (Solvene®300 EAP, courtesy of Solvay S.p.A. Milan). The copolymer shows a Curie temperature (T_c) of 103 °C and a melting temperature (T_m) of 145 °C, measured by Differential Scanning Calorimetry (DSC) analysis. As will be clarified afterward, these specific thermal features are crucial both for the fabrication and poling of the piezoelectric composite laminate.

The copolymer was dissolved at 20 wt % in a mixture of 55:45 wt % of acetone (AC) and dimethylformamide (DMF). The non-woven nanofibrous mat was fabricated with a four needle - drum collector electrospinning machine (Lab Unit, Spinbow®). Electrospinning process was carried out under the following optimized conditions: 0.8 ml/h flow rate per nozzle, 18 kV electric potential, 18 cm needle to collector distance, 0.2 m/s tangential speed, 20-24 °C temperature at 40÷50 % of relativity humidity (RH). Process was carried out for 8 hours to obtain an A3 size randomly oriented nanofibrous mat. In Fig. 1 a and b Scanning Electron Microscope (SEM) micrographs of the cross-section and morphology of the nanofibrous mat so obtained are shown, respectively. The measured mat thickness was 50 μm (evaluated with a digital indicator having a measuring pressure of 100 g/cm^2), while the areal weight was 16 g/m^2. The average fiber diameter, evaluated on 100 different fibers, was 340 ± 120 nm. The electrospinning process was stable and it has the potential to be scaled up at industrial level (e.g. by needleless technology), reducing the fabrication time by one or two orders of magnitude [25].
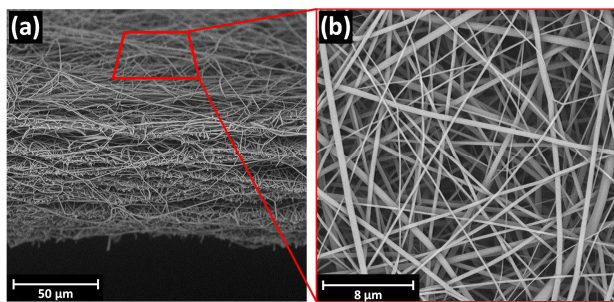

Fig. 1 SEM micrographs of the piezoelectric nanofibrous mat: (a) cross-section, (b) morphology.

2.1.2. Stacking sequence and Curing

The self-sensing laminate is composed of thin layers of aluminum (Al 2024-T3, 60 x 70 x 0.5 mm), interspersed with layers of woven Glass Fiber Reinforced Polymer (GFRP) prepreg (E-glass 8H Satin 300g/m^2 - epoxy matrix, VV300S - DT121H-34 DeltaPreg, 80 x 90 x ~0.22 mm) and the piezoelectric nanofibrous mat interleaved at the laminate midplane (80 x 90 x ~0.05 mm). The resulting stacking sequence is $[Al_1/(GFRP-0°)_4/ Al_1/(GFRP-0°)_2/Nano_1]_S$, as depicted in Fig. 2. The aluminum sheets, in addition to the structural function of increasing the impact resistance as occurs in standard GLARE laminates, have the electrical function of collecting the piezoelectric signal and shielding the sensor. For the sake of comparison, a laminate with the same stacking sequence of the self-sensing one (hereafter named Piezo) but lacking the nanofibrous mat (hereafter named Reference) was also fabricated.

Before stacking, the aluminum sheets were subjected to surface treatment by chemical etching in sulfuric acid/ferric sulfate solution (P-2 Etching according to ASTM D2651), to improve the adhesion with the epoxy matrix of the GFRP plies. Moreover, signal cables (430-FST, Micro-Measurements), coated with a Teflon jacket, to withstand the high temperatures of the composite curing cycle, were soldered on the aluminum sheets with a Sn/Cu 97/3 soldering paste specific for aluminum (Flux SN35). If difficulties in placing the signal cable should arise, due to the needs of trimming and/or constraining the edges of the composite structure, the cables can be let to come out from the laminate surface by making a small incision on the prepreg and aluminum sheets at the laminate edge, as proposed in [26].

After stacking, both Piezo and Reference laminates were cured in autoclave with a vacuum bag pressure of - 850 mbar and external pressure of 6 bar, using a custom 3 steps cure cycle (see graph of Fig. 3) made up of: (i) a 30 min isotherm @ 50 °C, (ii) a 120 min isotherm @ 100 °C, and (iii) a 60 min isotherm @ 150 °C, with 2 °C/min heating and cooling ramps. Step (i) was introduced to promote the impregnation of the nanofibrous mat, by decreasing the viscosity of the epoxy resin without significantly triggering the cross-linking. The second step (ii) allows the gradual cross-linking of the epoxy matrix in mild conditions, trying to avoid exotherm-triggered temperature overshot that might outgrow the melting temperature of the polymeric nanofibers, thus helping preserving their morphology. The third step (iii) completes the cross-linking of the epoxy resin and brings the glass transition temperature (T_g) over the Curie one (T_c). Despite the step (iii) temperature is above the melting temperature of PVDF-TrFE the nanofiber morphology is preserved because

the surrounding epoxy matrix has already a sufficient crosslinking degree to act as a mold. Note that in Fig. 3 the T_g reached by the resin at each step are also reported. The resulting final thickness of the cured laminate was 4.6 ± 0.05 mm.
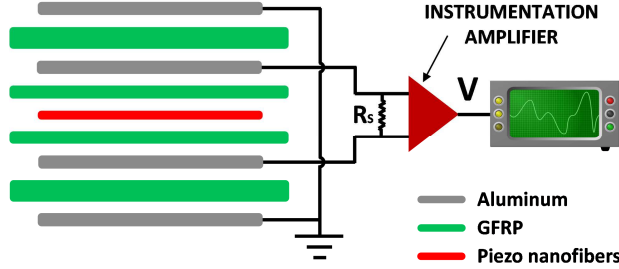

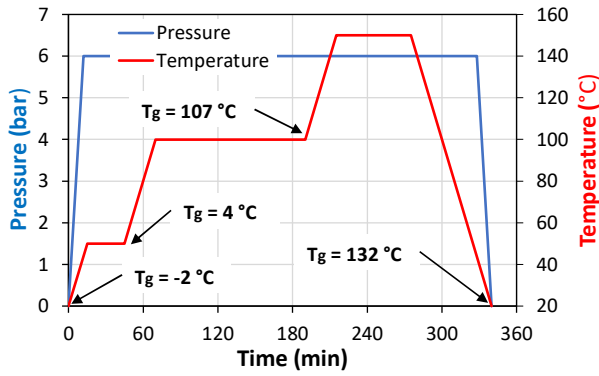*Fig. 2 Stacking sequence of the self-sensing GLARE laminate and electric connections.*

Fig. 3 Cure cycle of the self-sensing GLARE laminate.

2.1.3. Poling

Despite the ferroelectric nanofibrous mat could be self-polarized by the strong electric field employed in the electrospinning process [27] the preferential dipole orientation is lost during the subsequent curing of the composite laminate, which is carried out above the Curie temperature. Therefore, after curing, the self-sensing laminate with the embedded PVDF-TrFE nanofibrous mat was poled by applying an electric field of 6 kV/mm between the two inner electrodes (aluminum plies) at a temperature of 110 °C for 30 minutes and then cooling it down to room temperature at 2 °C/min, keeping the electric field on to stabilize the polar alignment. Finally, to remove any residual electrostatic charge induced by the electrospinning and poling processes, the laminate was left at 60 °C for 72 hours with short-circuited electrodes.

The polarization temperature of 110 °C was selected because is higher than the PVDF-TrFE Curie temperature ($T_c = 103$ °C), but at the same time lower than the glass transition temperature of the laminate epoxy matrix ($T_g = 132$ °C). Indeed, the mobility of the electric dipoles above Curie temperature increases and as consequence they can be aligned by applying a significantly lower poling electric field than the one necessary at room temperature (150 kV/mm as suggested by the supplier), reducing the risk of electrical breakdown. At the same time, the poling temperature was kept lower than the T_g temperature, above which the electric permittivity of the epoxy matrix would rapidly decrease [28], with consequent increases of the conductivity and, in turn, risk of electrical breakdowns. Another critical aspect in the poling process is the presence of voids which can trigger electrical discharges. Indeed, in preliminary samples cured out of autoclave, poling was not possible due to electrical discharges caused by a high void content.

The poling step represents the most critical aspect in the fabrication of the self-sensing laminate, because of the risk of electric breakdowns. However, if the poling temperature is kept between the Curie and Tg temperatures and composite voids are minimized (as in this case by using prepreg and autoclave technology), the piezoelectric nanofibers can be successfully polarized.

2.1.4. Signal conditioning

As shown in the diagram of Fig. 2, the electrical charges generated by the nanofibrous piezoelectric mat are collected by the two internal electrodes (aluminum sheets) of the laminate. While the two external aluminum plies of the laminates are connected to ground, to shield the sensor from triboelectric noise and external electromagnetic interferences.

The piezoelectric sensor, composed by the nanofiber embedded in the GFRP and the two aluminum electrodes, acts as a capacitor in parallel with a very high internal leakage resistance (thanks to the high permittivity of the GFRP). Therefore, the high impedance signal output of the piezoelectric sensor has to be converted by a pre-amplifier to a low impedance signal, suitable for the direct transmission to the acquisition system. The voltage amplifier is composed of an instrumentation amplifier (INA 118, Texas Instruments) with an impedance input of 10 GΩ and an interchangeable shunt resistor (varied from 1 kΩ to 1 GΩ) connected in parallel to the circuit, to tune the sensor electric response.

2.2. Low velocity Impact test

Non-destructive low-velocity impact tests were performed to investigate and optimize the electrical response of the self-sensing laminate to impact. For this purpose, a drop-weight tower was employed, built according to the ASTM D7136 standard, as showed in Fig. 4. The impactor had a total mass of 1.3 kg and a 12.7 mm diameter hemispherical steel tip, instrumented with a piezoelectric commercial load cell (208C05, PCB Piezotronics). The laminate was placed on a plane with a 60 x 50 mm pit (smaller than the standard one) and clamped with two harmonic steel strips, to avoid rebounds. The signal generated by the self-sensing laminate and the contact force measured by the impactor load cell were synchronously acquired at 100 kHz by means of an ADC converter (NI cDAQ 9171 combined with NI 9215, National Instrument). The electrical response of the laminate was investigated for different shunt resistances and with or without shielding. For this purpose, laminates were impacted multiple times keeping the maximum impact force lower than 0.5 kN to avoid damaging the laminate.
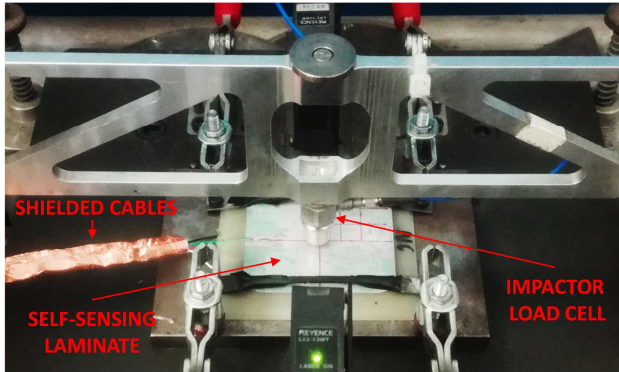

Fig. 4 Low velocity impact test set-up.

3. Results and discussion

3.1. Characterization of the embedded piezoelectric nanofibers

3.1.1. Morphology

The integration of the GLARE laminate with the piezoelectric nanofibrous mat was investigated by optical micrograph (Fig. 5a) and SEM (Fig. 5b and c) analyses of the cross-section. In Fig. 5a the resulting stacking

sequence of the self-sensing laminate can be observed, with the aluminum sheets, appearing as the white layers, interspersed with GFRP woven plies. Focussing on the laminate mid-plane (see Fig. 5 b and c), the piezoelectric nanofibrous mat embedded in the epoxy matrix can be observed. It is worth noting that PVDF-TrFE was removed by flushing the laminate in acetone, to help pointing out the empty traces left by the nanofibers, that clearly stand out from the matrix in the SEM micrographs. Fig. 5b clearly shows that the nanofibrous mat completely fills the matrix-rich interlayer between the upper and lower glass plies, by varying its thickness from 12 to 44 µm, to adapt to the weave of the fiberglass fabric. In the composite matrix, few voids can be observed, with a maximum diameter of 10 µm. However, their dimension did not compromise the poling process. Moreover, Fig. 5c shows that the nanofibrous mat is completely impregnated and integrated with the epoxy matrix. Generally, it can be noted that the contribution in volume and thickness of the piezoelectric nanofibrous mat on the GLARE laminate is negligible.
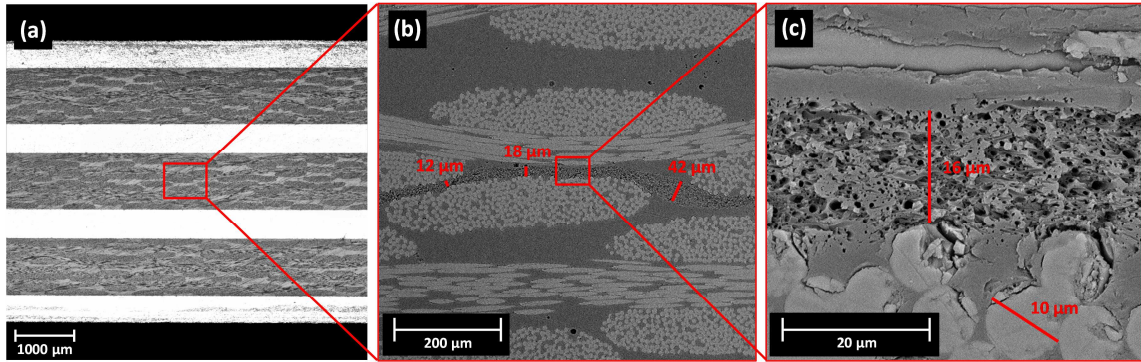

Fig. 5 Cross-section micrograph analysis of the piezoelectric nanofibrous mat integrated with GLARE laminate at different magnifications: (a) full laminate cross-section, (b) piezoelectric nanofibrous mat interlayer and (c) nanofibers.

3.1.2. Crystallinity

While PVDF homopolymer has several polymorphs including four known chain conformations, with the most common crystalline phase that shows no significant piezoelectric behavior, in PVDF-TrFE copolymer, on the contrary, the presence of the TrFE co-monomer helps the natural formation of the ferroelectric β crystalline phase, independently of the processing method [29,30]. The β-phase is, indeed, the one exhibiting the highest dipole moment and hence the most active piezoelectric phase. While the developed crystal phase (β-phase) is process-insensitive, the crystallinity degree χ_c and the average size of the crystallites, instead, may depend on the processing conditions, i.e. the cooling rate [31].
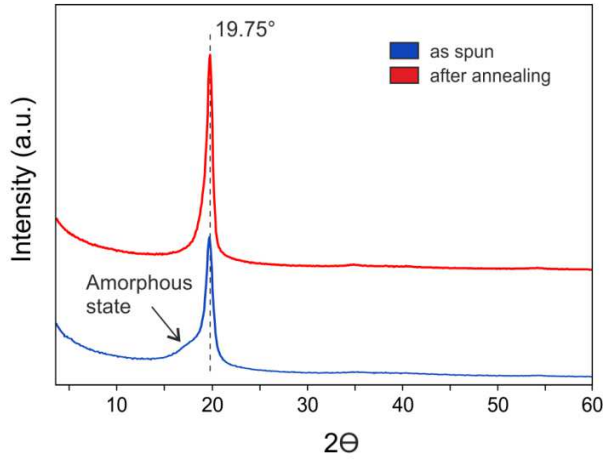
Fig. 6 WAXS diffractograms of PVDF-TrFE nanofibers: as-spun (blue) and after annealing at 150 °C for 1h (red) and cooling at 2 °C/min.

The Wide-angle X-ray scattering (WAXS) analysis was carried out in order to assess the actual crystal phase type and content in the obtained nanofibers: the diffraction pattern recorded for the "as spun" PVDF-TrFE (blue curve, Fig. 6) shows a reflection positioned at $2\Theta = 19.75°$, typical of sole electroactive β-phase crystal lattice [32]. Moreover, the as-spun nanofibers present a shoulder associated to a relevant amorphous phase fraction. Indeed, the high evaporation rate occurring during electrospinning process can act similarly to a high cooling rate for the polymeric melt (a similar shoulder is found in quenched PVDF-TrFE [32]). The annealing at 150 °C for 1h (red curve) significantly modifies the diffraction pattern of the nanofibrous membrane, with the crystal lattice 19.75° reflection that increases in intensity and definition and a contemporary reduction of the broad amorphous shoulder, denoting an improvement of the β-phase. The crystallinity degree, as calculated from the diffractograms deconvolution, also account for such an increase in β-phase content, with χ_c, that increases from 33% for as-spun nanofibers up to 52% for the annealed ones.

Note that the annealing conditions applied to the fibers are chosen to replicate the thermal condition at which the nanofibrous mat embedded in the composite are subjected during the curing cycle (see Fig. 3). Therefore, it can be assumed that the nanofibers embedded in the self-sensing laminate present an enhanced β-phase compared to as spun ones.

3.2. Piezoelectric response to impact

3.2.1. Shielding vs triboelectricity

During an impact, when the two colliding objects come into contact, a current flow may occur in between them. The current flow can be caused by the different electric potential between the two objects or the triboelectric charging generated by their friction [33]. This electric discharge, even if low, can interfere with the low voltage and high impedance piezoelectric signal. Moreover, the internal electrodes, due to the large area of the laminate, can behave as an antenna and collect the external electromagnetic interferences, thus disturbing the piezoelectric signal.

In the graphs of Fig. 7 the laminate electric response (red curve) was compared to the contact force measured by the impactor load cell (blue curve). In the top row is shown the Reference laminate behaviour while in the bottom row the Piezo one, with the external electrodes floating (left column) and grounded (right column). Theoretically, the reference laminate (GLARE without nanofibers) should be electrically inert, however, in the floating configuration a signal is recorded when the two colliding objects come into contact, which could be erroneously attributed to the contact force. Nevertheless, the signal does not fit the contact force curve and its shape, magnitude and sign were noticed to be random for multiple impacts with similar conditions. When the two external electrodes are grounded, instead, the signal is reduced by 3 orders of magnitude. This proves that the signal is generated by electrical disturbs and the external electrodes can shield them. Regarding the self-sensing laminate (Piezo), when the external electrodes are floating the piezoelectric signal is remarkably disturbed by the similar magnitude external electric noise. Instead, when the external electrodes are grounded the interference is shielded and the piezoelectric signal faithfully reproduces the contact force.
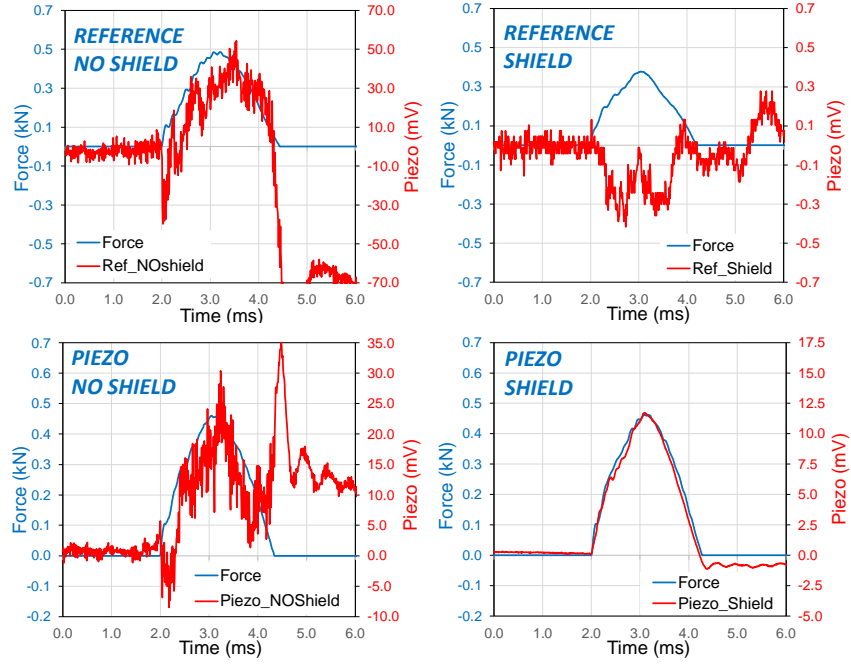
Fig. 7 Electric response (red curve) compared to the contact force measured by the impactor load cell (blue curve), for the Reference laminate (top row) and Piezo one (bottom row), with the external electrodes floating (left column) and grounded (right column) and a shunt resistance of 100 MΩ.

3.2.2. Signal proportionality vs shunt resistance

When the self-sensing laminate is subjected to impact, an electric charge proportional to the force magnitude

is developed in the piezoelectric element (composed by the nanofibers embedded in the GFRP and the two

aluminum electrodes) [34]. By virtue of the element capacitance this charge is stored in the element and is

prevented from leaking away, by the high leakage resistance of the piezoelectric element. However, the

impedance of the piezo element and the instrument amplifier input is not really infinite. Moreover, a shunt

resistance is necessary to discharge the time accumulated electric charges, coming from ambient noise. Hence

over time charges leak away and the piezoelectric signal loses its proportionality with the force magnitude.

In Fig. 8 the piezoelectric response of the self-sensing laminate (continuous red curve) generated during

impact is reported and compared to the contact force measured by the impactor commercial load cell (blue

curve), for different shunt resistance values. With 1 kΩ resistor the piezoelectric signal is too low to be

distinguished from the electric noise. By raising the resistance to 100 kΩ and then to 1 MΩ, the piezoelectric

signal magnitude increases and becomes detectable. However, the piezoelectric signal does not follow the

contact force trend, while it seems to be more proportional to its slope (time derivate). By further increasing the shunt resistance value from 1 MΩ to 1000 MΩ, the piezoelectric signal trend changes from semi-derivative to fully proportional, fitting better and better to the contact force curve. However, with a 1000 MΩ resistor the signal starts to drift (visible as a signal offset). Indeed, when the shunt resistance is too high, the electric charges coming from ambient noise cannot be dissipated. Therefore, a shunt resistance of 100 MΩ was chosen as the best compromise between signal proportionality and drifting.
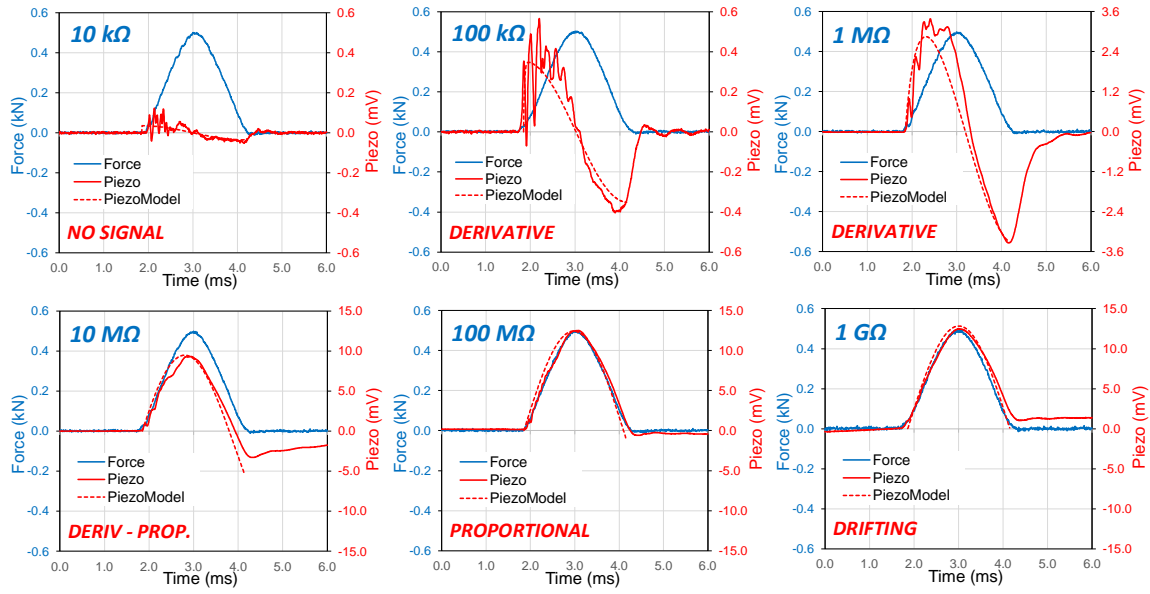

Fig. 8 Piezoelectric response of the self-sensing laminate (continuous red curve) compared to the contact force measured by the impactor load cell (blue curve) and the piezoelectric model estimated response (dotted red curve), for different shunt resistance values.

3.3. Electric model for the impact response of the self-sensing laminate

In Fig. 9 is shown the equivalent electric circuit of the self-sensing laminate connected to the voltage amplifier. In the circuit, the piezoelectric element can be modeled as a charge source Q_p, in parallel with a capacitor C_p and a very high internal leakage resistance which can be neglected [35]. The cable capacitance C_c is in parallel with the sensor one, while the low cable resistance can be neglected. The shunt resistor R_s is connected in parallel to the circuit. The impedance of the amplifier is, instead, high enough to be neglected. Therefore, according to Kirchhoff's law, the equivalent capacitance C is the sum of the piezo and cable capacitances in parallel ($C = Cp + Cc$), while the equivalent resistance R can be reduced to the shunt

13

resistance R_s. A capacitance of 182 pF and 19 pF was measured for the piezo element and the signal cable, respectively.
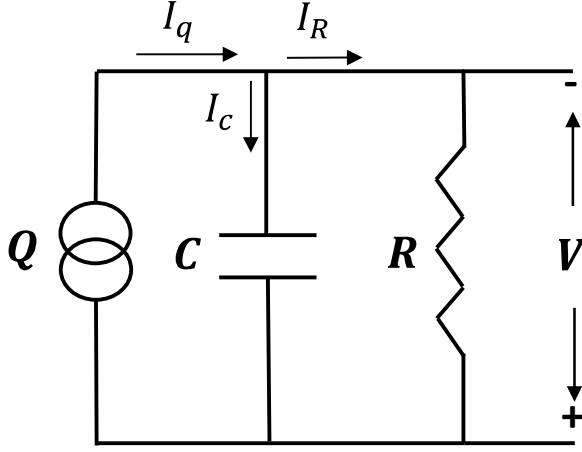

Fig. 9 Equivalent electric circuit of the self-sensing laminate connected to the voltage amplifier.

By applying Kirchhoff's laws and expressing the relationships of the electric components in complex form $(I_Q = dQ/dt = d_{33}\, dF/dt;\ I_C = V\, J\omega C;\ I_R = V/R)$, the circuit equation can be simply written as:

$$V(t) = \frac{R}{j\omega RC + 1}\, d_{33}\, \frac{dF(t)}{dt} \tag{1}$$

being the electric charges Q generated by the piezoelectric element proportional to the applied stress [34] and hence, in this case, to the impact force: $Q = d_{33}F$, with d_{33} the piezoelectric coefficient.

Under the assumption that non-linearities (indentation, membrane stiffness, damage) and mass of the laminate would be negligible, the impact can be modeled as a simple single degree of freedom spring-mass system [36], in which the impact force response is a half-sine wave: $F(t) = F\sin(\omega t)$, with $\omega = 2\pi/T$ and T equal to two times the impact duration.

Therefore, by solving Equation 1 in Laplace domain for a sine wave load and then anti transforming it back to the time domain, the piezoelectric voltage output for an impact load can be expressed as:

$$V(t) = \frac{Fd_{33}\omega R}{\omega^2 R^2 C^2 + 1}\left(-e^{-\frac{t}{RC}} + \cos(\omega t) + \omega RC\sin(\omega t)\right) \tag{2}$$

Equation 2 is composed of a transient component (exponential term) and a steady-state one (harmonic terms). It can be observed that for high time constant values ($\tau = RC$) compared to the impact time duration ($\omega = 2\pi/T$), the transient term and the first steady-state one can be neglected and the expression can be reduced to:

$$V(t) = \frac{F\, d_{33}}{C} \sin(\omega t) \tag{3}$$

Equation 3 shows that for high time constant values compared to the impact time duration, the piezoelectric voltage output becomes proportional to the contact force, confirming what was qualitatively observed in the graphs of Fig. 8. Moreover, the sensitivity (signal voltage / impact force ratio) of the self-sensing laminate results to be proportional to the piezoelectric coefficient d_{33}, independent by the resistance and inversely proportional to the capacitance C.

The unknown d_{33} coefficient was derived from the impact test results depicted in Fig. 8 for 100 MΩ resistance (high time constant value), by expressing Equation 3 as function of it. An equivalent piezoelectric coefficient of 5.12 x 10-3 pC/N was so obtained for the self-sensing laminate, which is 3 orders of magnitude lower than the one reported by the supplier for the pure PVDF-TrFE (22 pC/N). The remarkably lower value may be attributed to the piezoelectric nanofibers integration into the composite (see Fig. 5). In fact, being the laminate remarkably stiffer than the PVDF-TrFE polymer, the impact load directly transferred to the nanofibers is reduced and thus the generated electric charges.

In the graphs of Fig. 8 the piezoelectric voltage output estimated by the model (dotted red lines) for an impact duration of 2.35 ms, is compared to the experimental results (continuous red lines), for different shunt resistance values. As can be observed, the model curves have a similar trend to the experimental ones up to the impactor rebound because after that moment the impact force drop to zero, while the model hypothesized that the force after the initial transient continues as a steady state sine wave. In Fig. 10 the blue triangles represent the ratio between maximum voltage generated by the self-sensing laminate and the maximum force recorded during impact, for different shunt resistance values (experimental tests of Fig. 8), while the red curve is the ratio estimated by the piezoelectric model. As can be observed, the model fits the experimental results with good approximation. Moreover, the experimental results confirm what observed for Equation 3, that for high time constant values the sensitivity becomes independent of the resistance value.
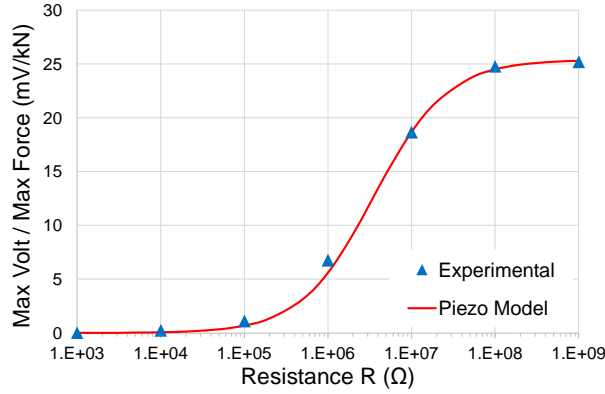
Fig. 10 Maximum output voltage – force ratio estimated by the electric model as function of the shunt resistance (red curve), compared to the ones obtained in the experimental tests of paragraph 3.2.2 (blue triangles).

As previously mentioned, according to Equation 3, the sensitivity is inversely proportional to the capacitance and, being the capacitance proportional to the laminate area, the latter is limited by the signal-to-noise ratio. Considering a noise level of 0.1 mV of the measuring chain and a resolution target of 0.1 kN, the maximum allowable area of the self-sensing laminate is 0.25 x 0.25 m^2. Over this value the electrodes, i.e. the internal aluminum sheets, have to be separated and the signals acquired independently. The multiple signals can be then conveyed to a common spot by cutting the internal aluminum sheets, mimicking the tracks of a PCB board. Moreover, the electrodes subdivision may be exploited for impact localization.

3.4. Sensor performances: linearity and spatial uniformity

Electrical performances of the self-sensing laminate were evaluated in terms of linearity (piezoelectric signal versus impact force) and spatial uniformity (sensor sensitivity versus impact position).

The sensor linearity has been evaluated by recording the piezoelectric voltage peak and contact force peak for impacts performed at different magnitude levels. Results are reported in the scatter plot of Fig. 11 and interpolated with a linear regression model with 95 % of probability confidence bands computed using the likelihood method as reported in ASTM E739. The sensitivity of the self-sensing laminate turns out to be 25.2 ± 1.7 mV/kN with a coefficient of determination R^2 equal to 0.999. It must be mentioned that the observed remarkable linearity (R^2) is quite common in piezoelectric sensors and also in a wide force range. The detected lower limit of the sensor sensitivity was of 0.05 kN and was attributed mostly to the inherent noise in

the measurement chain (electrodes, cables and amplification circuit). The measured sensitivity results to be adequate to detect an impact that can damage the composite, being generally in the kN scale. However, for the localization of the impact spot by triangulation, the sensitivity should be optimized (e.g., by varying the piezoelectric nanofibrous mat and GFRP thicknesses) in order to be able to detect elastic wave propagations into the laminate.

The self-sensing laminate should have the capability to detect an impact event on its whole surface for structural health monitoring purposes. Moreover, to provide a reliable response on the impact magnitude, and hence the consequent damage, the sensitivity should be as much homogeneous as possible on its surface. For this reason, the laminate was impacted with a magnitude of 0.5 kN at different points on its surface with a grid pattern of 3 x 3, 10 mm step between each point and origin in the laminate center. The measured sensitivity for each impact point is reported in the three-dimensional scatter plot of Fig. 11 b. The calculated sensitivity has a confidence interval of ± 1.1 mV/kN with 95 % confidence level, which corresponds to a relative error of ± 4.6 % and should be acceptable for structural health monitoring purposes. The measured relative error can be considered representative for larger laminates because the grid tested area is bigger than the unit dimensions of the glass fiber fabric texture and nanofibrous one.

By performing low-velocity impact tests, damage evolution can be experimentally correlated to the maximum impact force and therefore to the linear piezoelectric response of the self-sensing laminate. Hence, the SHM system can be alerted when the piezoelectric signal overcomes a certain threshold value [37,38].
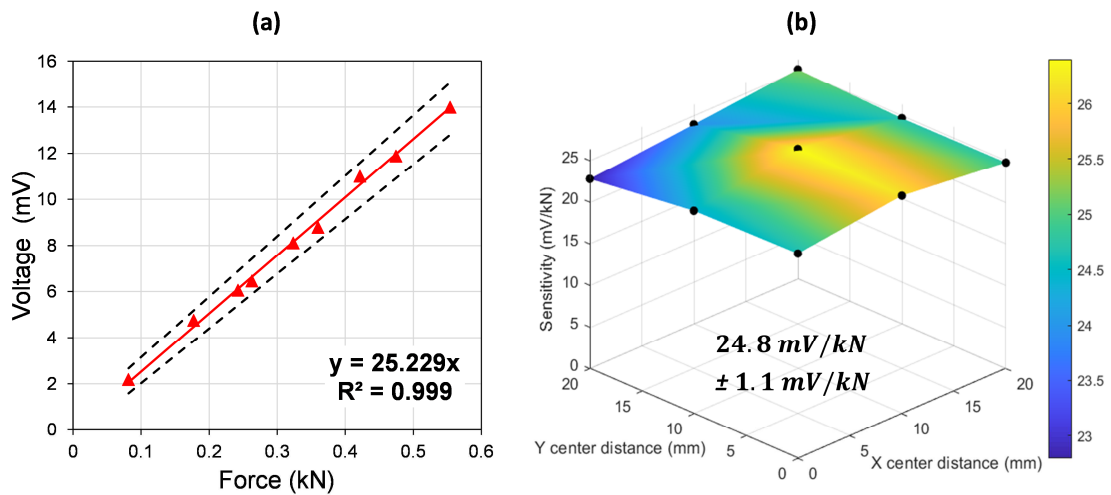

Fig. 11 (a) Sensor linearity: piezoelectric voltage peak versus contact force peak for impacts performed at different magnitude levels. (b) Spatial uniformity: sensitivity of the self-sensing laminate impacted at different points on its surface.

Conclusions

In this work, the integration of a nanostructured piezoelectric sensor, made of PVDF-TrFE nanofibers, into a composite laminate with aluminum sheets as electrodes has been achieved. Structurally, the resulting composite is a hybrid laminate known as Glass Laminate Aluminum Reinforced Epoxy (GLARE), consisting of aluminum sheets alternatively bonded to GFRP prepreg layers, functionalized with PVDF-TrFE interleaved nanofibrous mats. Such a nanostructured hybrid laminate becomes itself a piezoelectric sensor, capable to detect on its whole surface an impact load. This concept overcomes the issues related to the mechanical performance reduction due to the embedding of an extrinsic commercial sensor, which acts as damage triggering. The self-sensing laminate stacking sequence was designed to reduce the triboelectric and ambient noise. Moreover, a simple and compact electronic circuit, based on an instrumentation amplifier and a shunt resistance, was realized for the conditioning of the piezoelectric signal.

Non-destructive impact tests were performed using an instrumented drop-weight tower to investigate the real-time electrical response of the self-sensing laminate. A lumped electric model was applied to study and optimize the circuit electrical parameters. The piezoelectric signal response was studied for different shunt resistance values, and an optimized resistance value was found as the best compromise between signal proportionality and drifting. The sensor linearity, defined as sensor signal versus impact force, is of 0.99. While the spatial uniformity response, i.e. the sensor sensitivity versus different impact positions, showed a relative error of 4.6 %.

Future studies will focus on the evaluation of the impact strength of the self-sensing hybrid laminate functionalized by piezoelectric nanofibrous mat interleaving.

Declaration of competing interest

The authors declare that they have no known competing financial interests or personal relationships that could have appeared to influence the work reported in this paper.

Author CRediT contribution statement

Acknowledgments

References

[1] Hofmann P, Walch A, Dinkelmann A, Selvarayan SK, Gresser GT. Woven piezoelectric sensors as part of the textile reinforcement of fiber reinforced plastics. Compos Part A Appl Sci Manuf 2019. https://doi.org/10.1016/j.compositesa.2018.10.019.

[2] Cai J, Qiu L, Yuan S, Shi L, Liu P, Liang D. Structural Health Monitoring for Composite Materials. Compos. Their Appl., 2012. https://doi.org/10.5772/48215.

[3] Takeda N, Okabe Y, Kuwahara J, Kojima S, Ogisu T. Development of smart composite structures with small-diameter fiber Bragg grating sensors for damage detection: Quantitative evaluation of delamination length in CFRP laminates using Lamb wave sensing. Compos Sci Technol 2005. https://doi.org/10.1016/j.compscitech.2005.07.014.

[4]   Masmoudi S, El Mahi A, Turki S. Use of piezoelectric as acoustic emission sensor for in situ monitoring of composite structures. Compos Part B Eng 2015. https://doi.org/10.1016/j.compositesb.2015.06.003.

[5]   Konka HP, Wahab MA, Lian K. The effects of embedded piezoelectric fiber composite sensors on the structural integrity of glass-fiber-epoxy composite laminate. Smart Mater Struct 2012. https://doi.org/10.1088/0964-1726/21/1/015016.

[6]   Loayssa A. New Developments in Sensing Technology for Structural Health Monitoring. 2011. https://doi.org/10.1007/978-3-642-21099-0.

[7]   Li HN, Li DS, Song GB. Recent applications of fiber optic sensors to health monitoring in civil engineering. Eng Struct 2004. https://doi.org/10.1016/j.engstruct.2004.05.018.

[8]   Shivakumar K, Bhargava A. Failure mechanics of a composite laminate embedded with a fiber optic sensor. J Compos Mater 2005. https://doi.org/10.1177/0021998305048156.

[9]   Lin B, Giurgiutiu V. Modeling and testing of PZT and PVDF piezoelectric wafer active sensors. Smart Mater Struct 2006. https://doi.org/10.1088/0964-1726/15/4/022.

[10]   Lampani L, Sarasini F, Tirillò J, Gaudenzi P. Analysis of damage in composite laminates with embedded piezoelectric patches subjected to bending action. Compos Struct 2018. https://doi.org/10.1016/j.compstruct.2018.04.073.

[11]   Cheng J, Qian C, Zhao M, Lee SWR, Tong P, Zhang TY. Effects of electric fields on the bending behavior of PZT-5H piezoelectric laminates. Smart Mater Struct 2000. https://doi.org/10.1088/0964-1726/9/6/312.

[12]   Butler S, Gurvich M, Ghoshal A, Welsh G, Attridge P, Winston H, et al. Effect of embedded sensors on interlaminar damage in composite structures. J Intell Mater Syst Struct 2011. https://doi.org/10.1177/1045389X11414225.

[13]   De Rosa IM, Sarasini F. Use of PVDF as acoustic emission sensor for in situ monitoring of mechanical behaviour of glass/epoxy laminates. Polym Test 2010. https://doi.org/10.1016/j.polymertesting.2010.04.006.

[14]   Bae JH, Chang SH. Characterization of an electroactive polymer (PVDF-TrFE) film-type sensor for health monitoring of composite structures. Compos Struct 2015.

https://doi.org/10.1016/j.compstruct.2015.06.075.

[15] Tang B, Mommaerts J, Duncan RK, Duke JC, Dillard DA. Nondestructive evaluation of model

adhesive joints by PVDF piezoelectric film sensors. Exp Mech 1993.

https://doi.org/10.1007/BF02322485.

[16] Chrysochoidis NA, Gutiérrez E. Evaluation of the sensitivity and fatigue performance of embedded

piezopolymer sensor systems in sandwich composite laminates. Smart Mater Struct 2015.

https://doi.org/10.1088/0964-1726/24/2/025032.

[17] Zhang H, Bilotti E, Peijs T. The use of carbon nanotubes for damage sensing and structural health

monitoring in laminated composites: a review. Nanocomposites 2015.

https://doi.org/10.1080/20550324.2015.1113639.

[18] Kang I, Heung YY, Kim JH, Lee JW, Gollapudi R, Subramaniam S, et al. Introduction to carbon

nanotube and nanofiber smart materials. Compos Part B Eng 2006.

https://doi.org/10.1016/j.compositesb.2006.02.011.

[19] Kang I, Schulz MJ, Kim JH, Shanov V, Shi D. A carbon nanotube strain sensor for structural health

monitoring. Smart Mater Struct 2006. https://doi.org/10.1088/0964-1726/15/3/009.

[20] Spinelli G, Lamberti P, Tucci V, Vertuccio L, Guadagno L. Experimental and theoretical study on

piezoresistive properties of a structural resin reinforced with carbon nanotubes for strain sensing and

damage monitoring. Compos Part B Eng 2018. https://doi.org/10.1016/j.compositesb.2018.03.025.

[21] Vlot A, Gunnink W. Fibre Metal Laminates: an Introduction. 2001.

[22] Brugo T, Palazzetti R. The effect of thickness of Nylon 6,6 nanofibrous mat on Modes I–II fracture

mechanics of UD and woven composite laminates. Compos Struct 2016.

https://doi.org/10.1016/j.compstruct.2016.07.034.

[23] Zarei H, Brugo T, Belcari J, Bisadi H, Minak G, Zucchelli A. Low velocity impact damage

assessment of GLARE fiber-metal laminates interleaved by Nylon 6,6 nanofiber mats. Compos Struct

2017. https://doi.org/10.1016/j.compstruct.2017.01.079.

[24] Daelemans L, Van Paepegem W, De Clerck K. Effect of interleaved polymer nanofibers on the

properties of glass and carbon fiber composites. Fiber-Reinforced Nanocomposites Fundam. Appl.,

2020. https://doi.org/10.1016/b978-0-12-819904-6.00011-6.

[25]   Niu H, Lin T. Fiber generators in needleless electrospinning. J Nanomater 2012. https://doi.org/10.1155/2012/725950.

[26]   Feng T, Bekas D, Ferri Aliabadi MH. Active health monitoring of thick composite structures by embedded and surface-mounted piezo diagnostic layer. Sensors (Switzerland) 2020. https://doi.org/10.3390/s20123410.

[27]   Mandal D, Yoon S, Kim KJ. Origin of piezoelectricity in an electrospun poly(vinylidene fluoride-trifluoroethylene) nanofiber web-based nanogenerator and nano-pressure sensor. Macromol Rapid Commun 2011. https://doi.org/10.1002/marc.201100040.

[28]   Jilani W, Mzabi N, Gallot-Lavallée O, Fourati N, Zerrouki C, Zerrouki R, et al. Dielectric relaxations investigation of a synthesized epoxy resin polymer. Eur Phys J Plus 2015. https://doi.org/10.1140/epjp/i2015-15076-6.

[29]   Martins P, Lopes AC, Lanceros-Mendez S. Electroactive phases of poly(vinylidene fluoride): Determination, processing and applications. Prog Polym Sci 2014. https://doi.org/10.1016/j.progpolymsci.2013.07.006.

[30]   Kepler RG, Anderson RA. Ferroelectric polymers. Adv Phys 1992. https://doi.org/10.1080/00018739200101463.

[31]   Maccaferri E, Mazzocchetti L, Benelli T, Brugo TM, Zucchelli A, Giorgini L. Rubbery nanofibers by co-electrospinning of almost immiscible NBR and PCL blends. Mater Des 2020. https://doi.org/10.1016/j.matdes.2019.108210.

[32]   Xia W, Xu Z, Zhang Q, Zhang Z, Chen Y. Dependence of dielectric, ferroelectric, and piezoelectric properties on crystalline properties of p(VDF-co-TrFE) copolymers. J Polym Sci Part B Polym Phys 2012. https://doi.org/10.1002/polb.23125.

[33]   Wang ZL, Wang AC. On the origin of contact-electrification. Mater Today 2019. https://doi.org/10.1016/j.mattod.2019.05.016.

[34]   Piezoelectric sensorics: force, strain, pressure, acceleration and acoustic emission sensors, materials and amplifiers. Choice Rev Online 2002. https://doi.org/10.5860/choice.40-0924.

[35]   Serridge M, Licht TR. Piezoelectric accelerometers and Vibration Preamplifiers - Theory and Application Handbook. Bruel & Kjaer; 1987.

[36]   Abrate S. Impact on Composite Structures. 1998. https://doi.org/10.1017/cbo9780511574504.

[37]   Fu H, Sharif Khodaei Z, Aliabadi MHF. An Event-Triggered Energy-Efficient Wireless Structural
        Health Monitoring System for Impact Detection in Composite Airframes. IEEE Internet Things J
        2019. https://doi.org/10.1109/JIOT.2018.2867722.

[38]   Fu H, Sharif Khodaei Z, Aliabadi MH. An energy efficient wireless module for on-board aircraft
        impact detection, 2019. https://doi.org/10.1117/12.2513534.

Figure captions

Fig. 1 SEM micrographs of the piezoelectric nanofibrous mat: (a) cross-section, (b) morphology.

Fig. 2 Stacking sequence of the self-sensing GLARE laminate and electric connections.\

Fig. 3 Cure cycle of the self-sensing GLARE laminate.

Fig. 4 Low velocity impact test set-up.

Fig. 5 Cross-section micrograph analysis of the piezoelectric nanofibrous mat integrated with GLARE laminate at different magnifications: (a) full laminate cross-section, (b) piezoelectric nanofibrous mat interlayer and (c) nanofibers.

Fig. 6 WAXS diffractograms of PVDF-TrFE nanofibers: as-spun (blue) and after annealing at 150 °C for 1h (red) and cooling at 2 °C/min.

Fig. 7 Electric response (red curve) compared to the contact force measured by the impactor load cell (blue curve), for the Reference laminate (top row) and Piezo one (bottom row), with the external electrodes floating (left column) and grounded (right column) and a shunt resistance of 100 MΩ.

Fig. 8 Piezoelectric response of the self-sensing laminate (continuous red curve) compared to the contact force measured by the impactor load cell (blue curve) and the piezoelectric model estimated response (dotted red curve), for different shunt resistance values.

Fig. 9 Equivalent electric circuit of the self-sensing laminate connected to the voltage amplifier.

Fig. 10 Maximum output voltage – force ratio estimated by the electric model as function of the shunt resistance (red curve), compared to the ones obtained in the experimental tests of paragraph 3.2.2 (blue triangles).

Fig. 11 (a) Sensor linearity: piezoelectric voltage peak versus contact force peak for impacts performed at different magnitude levels. (b) Spatial uniformity: sensitivity of the self-sensing laminate impacted at different points on its surface.

Author CRediT contribution statement

Tommaso Maria Brugo: Conceptualization, Methodology, Investigation, Formal analysis, Writing - original draft.

Emanuele Maccaferri: Investigation, Formal analysis, Writing - original draft. **Davide Cocchi:** Investigation, Writing - original draft, Writing - Review & Editing. **Davide Fabiani:** Methodology. **Laura Mazzocchetti:** Writing - Review & Editing. **Loris Giorgini:** Project administration. **Andrea Zucchelli:** Conceptualization, Supervision, Project administration.